Envelope Protein Glycosylation Mediates Zika Virus Pathogenesis

Derek L. Carbaugh,[a] Ralph S. Baric,[a,b] Helen M. Lazear[a]

[a]Department of Microbiology and Immunology, University of North Carolina at Chapel Hill, Chapel Hill, North Carolina, USA
[b]Department of Epidemiology, University of North Carolina at Chapel Hill, Chapel Hill, North Carolina, USA

ABSTRACT Zika virus (ZIKV) is an emerging mosquito-borne flavivirus. Recent ZIKV outbreaks have produced serious human disease, including neurodevelopmental malformations (congenital Zika syndrome) and Guillain-Barré syndrome. These outcomes were not associated with ZIKV infection prior to 2013, raising the possibility that viral genetic changes could contribute to new clinical manifestations. All contemporary ZIKV isolates encode an N-linked glycosylation site in the envelope (E) protein (N154), but this glycosylation site is absent in many historical ZIKV isolates. Here, we investigated the role of E protein glycosylation in ZIKV pathogenesis using two contemporary Asian-lineage strains (H/PF/2013 and PRVABC59) and the historical African-lineage strain (MR766). We found that glycosylated viruses were highly pathogenic in $Ifnar1^{-/-}$ mice. In contrast, nonglycosylated viruses were attenuated, producing lower viral loads in the serum and brain when inoculated subcutaneously but remaining neurovirulent when inoculated intracranially. These results suggest that E glycosylation is advantageous in the periphery but not within the brain. Accordingly, we found that glycosylation facilitated infection of cells expressing the lectins dendritic cell-specific intercellular adhesion molecule-3-grabbing nonintegrin (DC-SIGN) or DC-SIGN-related (DC-SIGNR), suggesting that inefficient infection of lectin-expressing leukocytes could contribute to the attenuation of nonglycosylated ZIKV in mice.

IMPORTANCE It is unclear why the ability of Zika virus (ZIKV) to cause serious disease, including Guillain-Barré syndrome and birth defects, was not recognized until recent outbreaks. One contributing factor could be genetic differences between contemporary ZIKV strains and historical ZIKV strains. All isolates from recent outbreaks encode a viral envelope protein that is glycosylated, whereas many historical ZIKV strains lack this glycosylation. We generated nonglycosylated ZIKV mutants from contemporary and historical strains and evaluated their virulence in mice. We found that nonglycosylated viruses were attenuated and produced lower viral loads in serum and brains. Our studies suggest that envelope protein glycosylation contributes to ZIKV pathogenesis, possibly by facilitating attachment to and infection of lectin-expressing leukocytes.

KEYWORDS Zika virus, flavivirus, $Ifnar1^{-/-}$ mouse, glycosylation, DC-SIGN, CD209, DC-SIGNR, L-SIGN, CD209L

Zika virus (ZIKV) is an emerging flavivirus primarily transmitted by mosquitos. Most ZIKV infections are asymptomatic, with approximately 20% resulting in self-limiting illness, including maculopapular rash, fever, and/or conjunctivitis (1, 2). Historically, ZIKV was not associated with significant human disease. However, recent ZIKV outbreaks have featured new clinical manifestations. The 2013–2014 ZIKV outbreak in French Polynesia was associated with an increase in Guillain-Barré syndrome, an autoimmune neuropathy that can result in weakness, paralysis, and death (2–4). The

subsequent detection of ZIKV in Brazil in 2015 and the rapid spread of ZIKV to many countries in the Americas (5–8) has revealed that ZIKV infection during pregnancy can cause a broad range of congenital malformations termed congenital Zika syndrome (2, 9, 10).

ZIKV is grouped into two major phylogenetic lineages, African and Asian. All contemporary American strains belong to the Asian lineage, and genetic analyses support a model of a single introduction of ZIKV to Brazil from the South Pacific (7, 8, 11). It is unknown why severe disease manifestations, such as congenital Zika syndrome, were revealed only during the most recent ZIKV outbreak, but nonexclusive explanations include (i) the ability of a large outbreak with good surveillance to reveal rare outcomes, (ii) different host genetic or immune status in Latin America compared to regions where ZIKV circulated previously, and (iii) genetic changes in ZIKV strains resulting in altered tropism and/or enhanced pathogenesis (12). Amino acid substitutions that may contribute to the increased rate of transmission and/or pathogenicity have been identified by comparative genomic and phylogenetic analyses (13–15). Differences in nonstructural protein 1 (NS1) and premembrane protein (prM) have been associated experimentally with enhanced transmission or virulence of American strains (11, 16–18). These analyses also have revealed a difference in the N-linked glycosylation motif (N-X-S/T) at amino acid 154 of the ZIKV envelope (E) protein. Many African-lineage ZIKV isolates lack the glycosylation signal due to either a 4- to 6-amino-acid deletion or a change of T to I at position 156, whereas all Asian-lineage strains, including ones from recent outbreaks, contain an intact glycosylation signal (19, 20). This is significant because N-linked glycosylation on E is associated with enhanced mosquito transmission and/or increased vertebrate virulence of other flaviviruses, including West Nile virus (WNV), Japanese encephalitis virus (JEV), tick-borne encephalitis virus, and others (21–30).

In this study, we investigated the role of E glycosylation in ZIKV pathogenesis across Asian- and African-lineage ZIKV strains. We used site-directed mutagenesis to ablate the glycosylation motif with a single amino acid substitution (N154Q) in a previously described infectious clone of the Asian-lineage ZIKV strain H/PF/2013 (31). We generated a new infectious clone of another widely used Asian-lineage ZIKV strain, PRVABC59, and ablated the glycosylation motif with either an N154Q or a T156I substitution. Finally, we used our previously reported infectious clones derived from the prototype African-lineage ZIKV strain MR766 TVP 14270 with a 4-amino-acid deletion ablating the glycosylation site, as well as mutants with restoration of the glycosylation signal or the 4 amino acids restored with a T156I mutation ablating the glycosylation signal (31). We show that mutant viruses lacking the E glycosylation are avirulent in $Ifnar1^{-/-}$ mice and are attenuated in overall replication *in vivo*. We also show that the lectins dendritic cell-specific intercellular adhesion molecule-3-grabbing nonintegrin (DC-SIGN, CD209) and DC-SIGN-related (DC-SIGNR, CD209L, L-SIGN) facilitate infection of glycosylated virus in cell culture. Our results indicate that N-linked glycosylation of the ZIKV E protein mediates infection and pathogenesis and suggest that the glycan may enhance infectivity via cell surface lectins.

RESULTS

N154Q mutation ablates E glycosylation. To evaluate the role of E glycosylation in ZIKV infection, we used site-directed mutagenesis to introduce a single amino acid substitution, N154Q, that ablates the glycosylation motif (N-X-S/T) in a previously described infectious clone of ZIKV strain H/PF/2013 (Fig. 1A) (31). Consensus sequencing of virus released from electroporated Vero cells confirmed the two engineered nucleotide changes (Fig. 1B). We compared the growth of the H/PF/2013 isolate, a wild-type (WT) clone, and the N154Q mutant in Vero cells and found equivalent replication kinetics (Fig. 1C). To verify the glycosylation status of the viral E protein, we immunoprecipitated lysates from infected Vero cells with monoclonal antibody (MAb) 1M7. We digested the immunoprecipitates with peptide N-glycosidase F (PNGase F) to remove all N-linked carbohydrates. When probed by Western blotting with MAb 4G2,
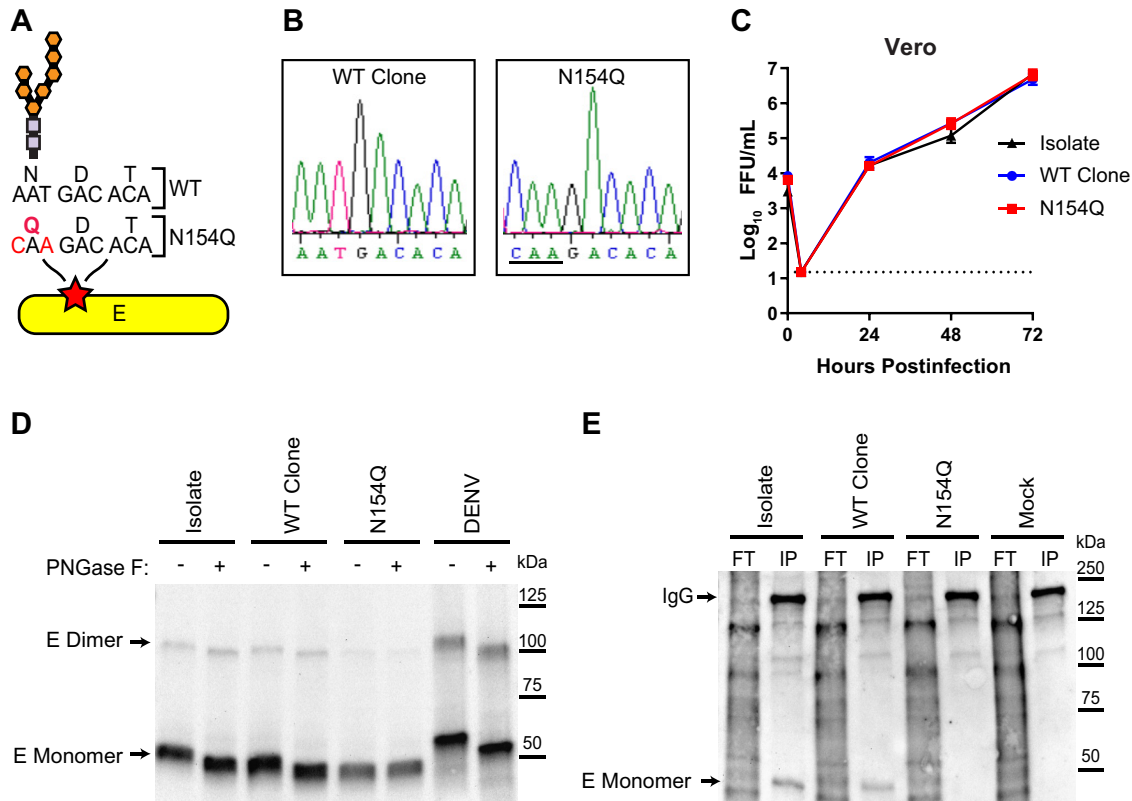
FIG 1 E glycosylation is not required for ZIKV replication. (A) ZIKV envelope protein, depicting the nucleotide and amino acid residues of the glycosylation site, and N154Q mutation. (B) Sequence chromatograms of E protein glycosylation site of wild-type (WT) and N154Q viruses. (C) Vero cells were infected at an MOI of 0.01 with ZIKV H/PF/2013 isolate, WT clone, or N154Q mutant. Viruses in culture supernatants were titrated by focus-forming assay. Data shown are the mean values ± standard errors of the means (SEM) of 9 samples from 3 independent experiments. (D and E) E proteins were immunoprecipitated with MAb 1M7 from lysates of Vero cells infected with ZIKV H/PF/2013 isolate, WT clone, N154Q mutant, or DENV. (D) Lysates were treated with PNGase F, separated by nonreducing SDS-PAGE, and probed with MAb 4G2. (E) Lysates were separated by nonreducing SDS-PAGE and probed with biotinylated concanavalin A to detect glycans. FT, flow-through; IP, immunoprecipitate.

E protein from H/PF/2013 isolate virus and WT infectious clones exhibited a lower molecular weight after PNGase F treatment, indicating glycan cleavage (Fig. 1D). However, the size of the N154Q E protein was unaffected by PNGase F digestion, indicating that the mutant E protein was not glycosylated. Compared to that of ZIKV, dengue virus (DENV) E protein exhibited a greater size shift upon PNGase F digestion, as expected, because DENV E has two glycosylation sites (N67 and N153) (32). We further confirmed the glycosylation state of the viral E protein by lectin blotting, using biotinylated concanavalin A (ConA), a mannose/glucose binding lectin, to probe E protein immunoprecipitated from infected Vero cells. Consistent with the results from PNGase F digestion, the H/PF/2013 isolate and WT clone E proteins were detected by ConA, whereas the N154Q E protein was not (Fig. 1E).

ZIKV E N154Q is attenuated upon subcutaneous but not intracranial inoculation. We next evaluated the virulence of the N154Q mutant in mice. ZIKV does not replicate efficiently in WT C57BL/6 mice because ZIKV NS5 protein does not antagonize mouse STAT2 (33, 34). Thus, mouse models of ZIKV pathogenesis typically employ mice lacking interferon alpha/beta (IFN-$\alpha\beta$) signaling, such as through genetic loss of the IFN-$\alpha\beta$ receptor (*Ifnar1$^{-/-}$*) (35, 36). To evaluate the role of E glycosylation in ZIKV pathogenesis, we infected 5- to 6-week-old *Ifnar1$^{-/-}$* mice with 1×10^3 focus-forming units (FFU) of WT or N154Q virus by a subcutaneous route in the footpad and evaluated weight loss and lethality (Fig. 2A and B). Mice infected with WT clone virus began losing weight at 4 days postinfection (dpi), and all mice succumbed by 7 dpi, consistent with previous studies with the H/PF/2013 isolate virus (35). In contrast, mice infected with
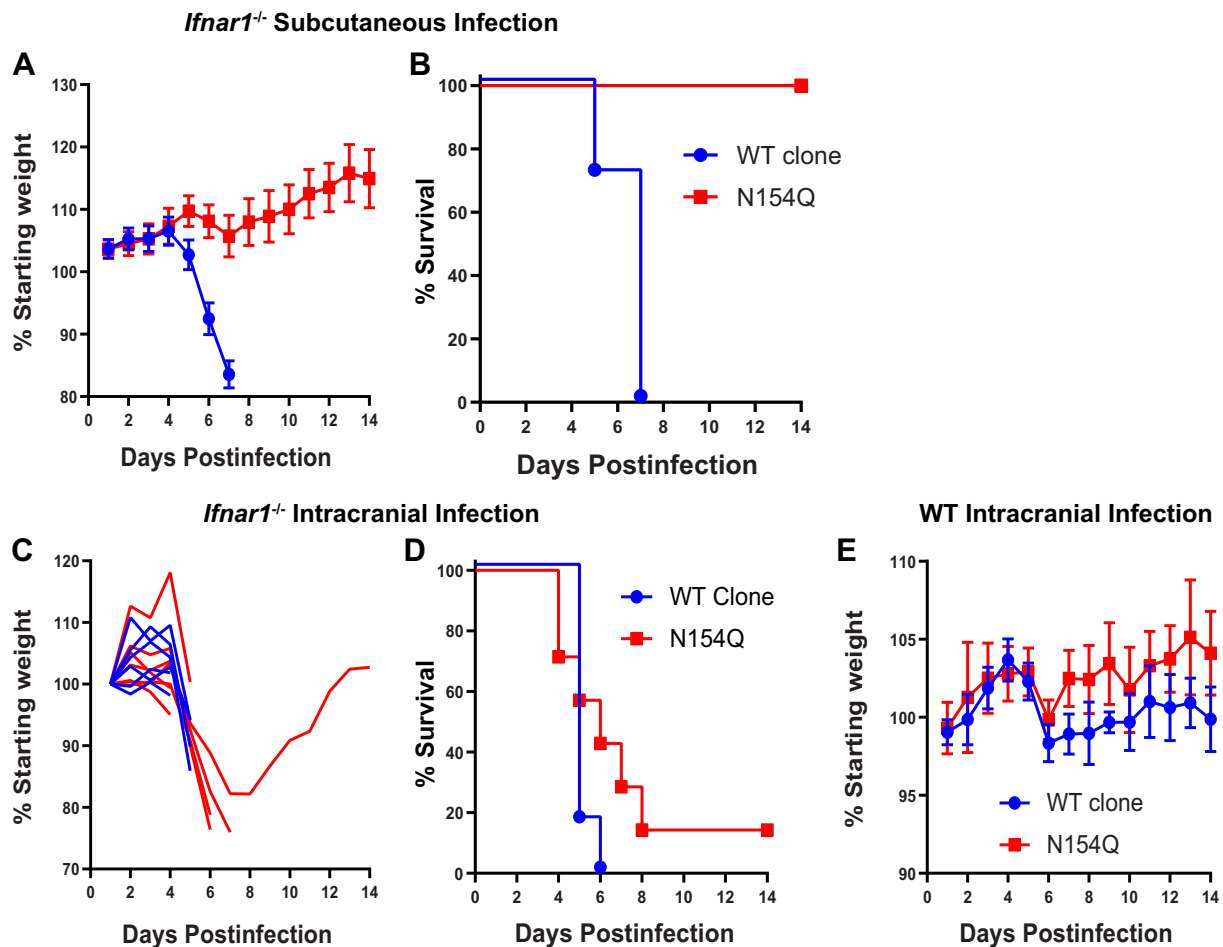
FIG 2 ZIKV E N154Q is attenuated upon subcutaneous but not intracranial inoculation. Five- to six-week-old *Ifnar1*$^{-/-}$ or wild-type (WT) mice were inoculated with 1×10^3 FFU of ZIKV strain H/PF/2013 WT clone or N154Q mutant by a subcutaneous (A and B) or intracranial (C to E) route. Mice were weighed daily, and weights are expressed as percentages of body weight prior to infection. Results shown are the mean values $\pm$ SEM of 6 to 8 *Ifnar1*$^{-/-}$ mice or 3 WT mice per virus from two or three independent experiments. Lethality was monitored for 14 days.

the N154Q virus lost weight from 5 to 7 dpi but recovered, and all mice survived. Studies with ZIKV and other flaviviruses have identified a role for E glycosylation in neuroinvasion (23, 24, 37), so we tested whether the N154Q mutant regained virulence if the blood-brain barrier was bypassed. We infected WT and *Ifnar1*$^{-/-}$ mice with 1×10^3 FFU of WT or N154Q virus by intracranial inoculation and found that both viruses caused equivalent weight loss and lethality (Fig. 2C to E). Six of 7 *Ifnar1*$^{-/-}$ mice infected with the N154Q mutant died, while 1 mouse lost weight and recovered. WT mice lost weight from 4 to 6 dpi, but all mice recovered and all mice survived infection with both viruses. Overall, these results indicate that ZIKV N154Q remained neurovirulent, even though this virus was attenuated via a subcutaneous inoculation route.

ZIKV E N154Q has impaired replication *in vivo*. Since the ZIKV N154Q virus was avirulent following subcutaneous inoculation but lethal upon intracranial inoculation, we tested whether E glycosylation mediated neuroinvasion, as well as invasion into other specialized tissue compartments, such as the eyes and testes, compared to peripheral tissues such as blood and the spleen. We infected 5-week-old *Ifnar1*$^{-/-}$ mice with 1×10^3 FFU of WT or N154Q virus via subcutaneous footpad inoculation and measured viral loads in the serum at 2, 4, and 6 dpi (Fig. 3A) and viral loads in tissues at 6 dpi by reverse transcription-quantitative PCR (qRT-PCR) (Fig. 3B to E). Compared to the WT virus, ZIKV N154Q produced lower viral loads in the serum at all time points, as well as reduced viral loads in the brain and eyes. In contrast, viral loads in the spleen
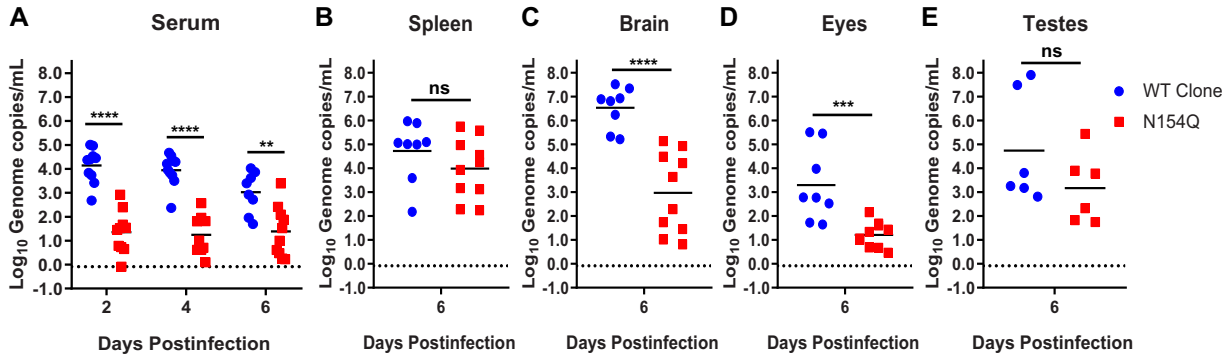
FIG 3 N154 glycosylation mediates ZIKV infection in mice. Five- to six-week-old *Ifnar1*−/− mice were inoculated with 1 × 10³ FFU of ZIKV strain H/PF/2013 WT clone or N154Q mutant by a subcutaneous route in the footpad. (A) Blood was collected at 2, 4, and 6 days after infection, and ZIKV RNA in serum was measured by qRT-PCR. (B to E) Mice were euthanized 6 days after infection and perfused, and tissues were harvested. ZIKV RNA in tissue was measured by qRT-PCR. **, P < 0.01; ***, P < 0.001; ****, P < 0.0001; ns, not significant (unpaired 2-tailed *t* test).

and testes were not affected by E glycosylation. These results indicate that ZIKV H/PF/2013 N154Q, lacking the E glycosylation, was attenuated and produced lower viremia, which could contribute to lower viral loads detected in some tissues.

Low levels of ZIKV detected in the brains of N154Q-infected mice could result from delayed or inefficient neuroinvasion by the nonglycosylated virus. Alternatively, the attenuated mutant could revert in the periphery, producing WT virus that infects the brain. To distinguish these possibilities, we extracted RNA from brains 6 days after footpad inoculation with ZIKV N154Q and evaluated viral E sequences by Sanger sequencing. Based on sequencing chromatograms, 7 of 10 brains contained a mixture of WT and N154Q virus, 1 brain contained predominantly WT virus, and 2 brains contained predominantly N154Q virus. To determine whether the N154Q mutant was stable in the periphery, we performed Sanger sequencing on RNA extracted from serum 2 days after infection with ZIKV N154Q. We found that serum from 2 of 5 mice sequenced contained a mixture of WT and N154Q virus, while the N154Q mutation was maintained in 3 mice. We next sequenced virus from brains harvested 5 to 8 days after intracranial inoculation with ZIKV N154Q and found that the N154Q mutation was maintained in 6 of 6 mice. Altogether, these data suggest selection favoring glycosylated virus in peripheral tissues but not within the brain of ZIKV-infected *Ifnar1*−/− mice.

Asian- and African-lineage strains lacking the E glycosylation are attenuated. ZIKV strain H/PF/2013 was isolated from an outbreak in French Polynesia in 2013, which preceded the emergence of ZIKV in the Americas and only retrospectively was associated with cases of congenital Zika syndrome (38–41). Since other reports of a role for E glycosylation in mediating ZIKV virulence used an African-lineage strain (37) or a Cambodian strain from 2010 (42), we sought to determine if glycosylation mediated similar effects on virulence and tissue invasiveness in a contemporary ZIKV strain from Latin America. We generated a new infectious clone of another widely used contemporary Asian-lineage strain, PRVABC59 (Puerto Rico, 2015) (Fig. 4A) (43). Due to the high nucleotide identity between H/PF/2013 and PRVABC59 (>99%), we were able to use the same restriction endonuclease sites to partition the viral genome across four plasmids, as previously described (31). Following digestion, ligation, *in vitro* transcription, and electroporation into Vero cells, infectious virus was recovered. The virus was passaged once on Vero cells, and titers were determined by focus-forming assay (FFA). The open reading frame of the WT infectious clone was sequenced, and we confirmed that no new mutations were introduced compared to the reference genome sequence for this strain (accession number KU501215). We used site-directed mutagenesis to introduce a single amino acid substitution (N154Q) to ablate the glycosylation motif (N-X-S/T). We also made a second mutant virus with the glycosylation motif ablated by a T156I mutation, as this variant has been detected in ZIKV strains isolated from mosquitos in Africa in the 1970s and 1980s (20, 44). The region surrounding the
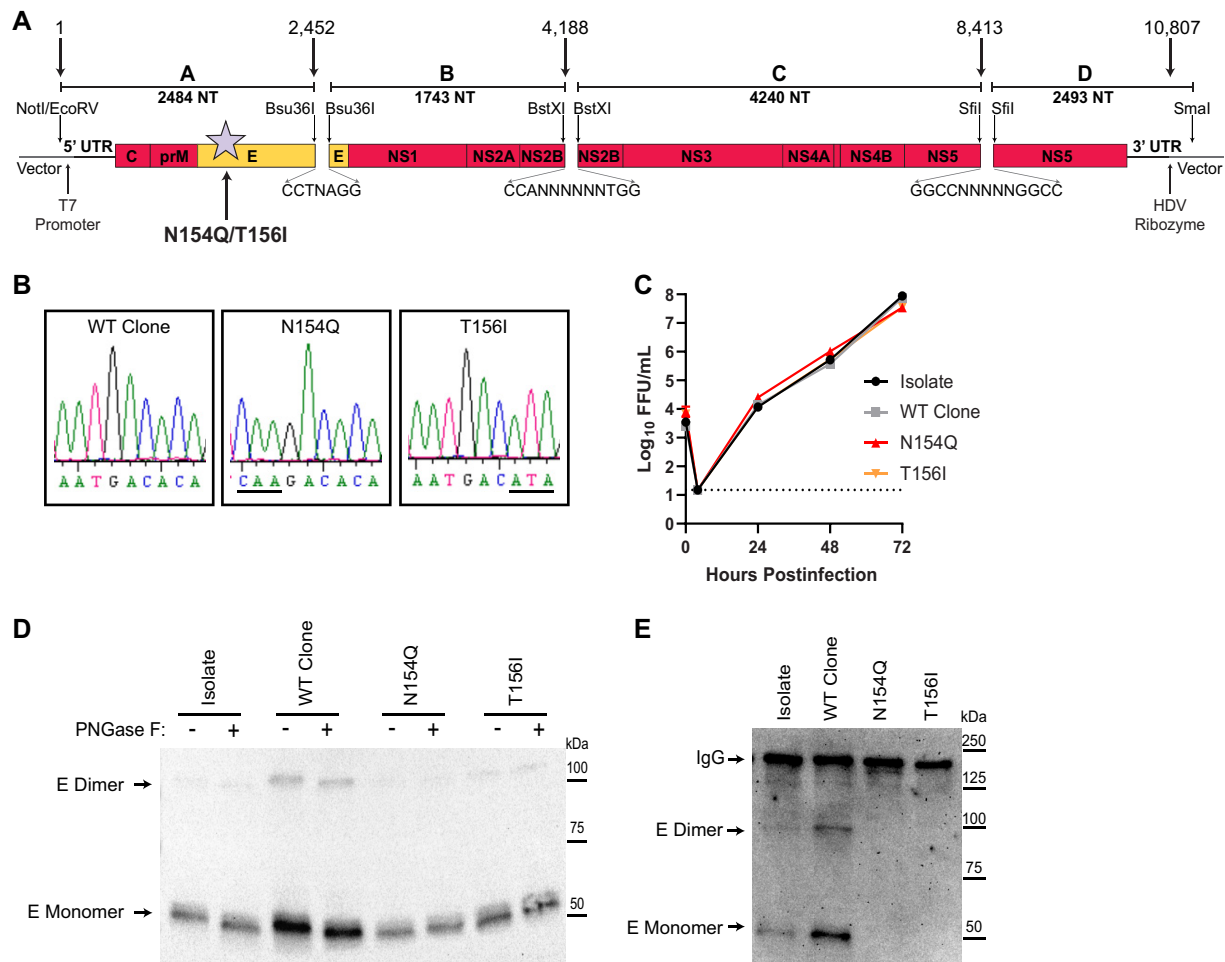
FIG 4 Generating an infectious clone of ZIKV PRVABC59 and nonglycosylated mutants. (A) An infectious clone of ZIKV strain PRVABC59 was generated using a system that divides the viral genome into 4 fragments flanked by the indicated restriction endonuclease sites. Numbers above fragments indicate nucleotide position in the viral genome. T7 promoter and a hepatitis delta virus (HDV) ribozyme sequences flank the genome. (B) Sequence chromatograms of E protein glycosylation site of WT, N154Q, or T156I clone. (C) Vero cells were infected at an MOI of 0.01 with ZIKV PRVABC59 isolate, WT clone, N154Q mutant, or T156I mutant. Viruses in culture supernatants were titrated by focus-forming assay. Data shown are the mean values ± SEM of 9 samples from 3 independent experiments. (D and E) E proteins were immunoprecipitated with MAb 1M7 from lysates of Vero cells infected with ZIKV PRVABC59 isolate, WT clone, N154Q mutant, or T156I mutant. (D) Lysates were treated with PNGase F, separated by nonreducing SDS-PAGE, and probed with MAb 4G2. (E) Lysates were separated by nonreducing SDS-PAGE and probed with biotinylated lectin concanavalin A.

introduced mutation was sequenced (Fig. 4B). All four viruses replicated equivalently in Vero cells (Fig. 4C). We performed PNGase F digestion (Fig. 4D) and lectin blotting (Fig. 4E) on immunoprecipitated E protein from Vero cells infected with PRVABC59 isolate, WT clone, N154Q mutant, and T156I mutant viruses to confirm the E glycosylation state. PNGaseF digestion produced a size shift for the PRVABC59 isolate and WT clone E proteins but not for the two mutants (Fig. 4D). Lectin blotting showed a band for the PRVABC59 isolate and the WT clone E proteins, but no band was detected for the two mutants lacking the E glycosylation (Fig. 4E). These results indicate that ZIKV PRVABC59 isolate and WT clone E protein are glycosylated and that this glycosylation is ablated by either N154Q or T156I mutations.

We next tested the virulence of the PRVABC59 viruses in *Ifnar1*^{−/−} mice. We infected 5- to 6-week-old mice with 1×10^3 FFU of PRVABC59 isolate, WT clone, N154Q, or T156I viruses via subcutaneous footpad inoculation and measured viral loads in the serum at 2, 4, and 6 dpi (Fig. 5A) and tissues at 6 dpi by qRT-PCR (Fig. 5B to E). The WT clone produced viral loads similar to those of the isolate virus. However, both nonglycosylated mutants produced lower viral loads than did WT viruses at all time points in the
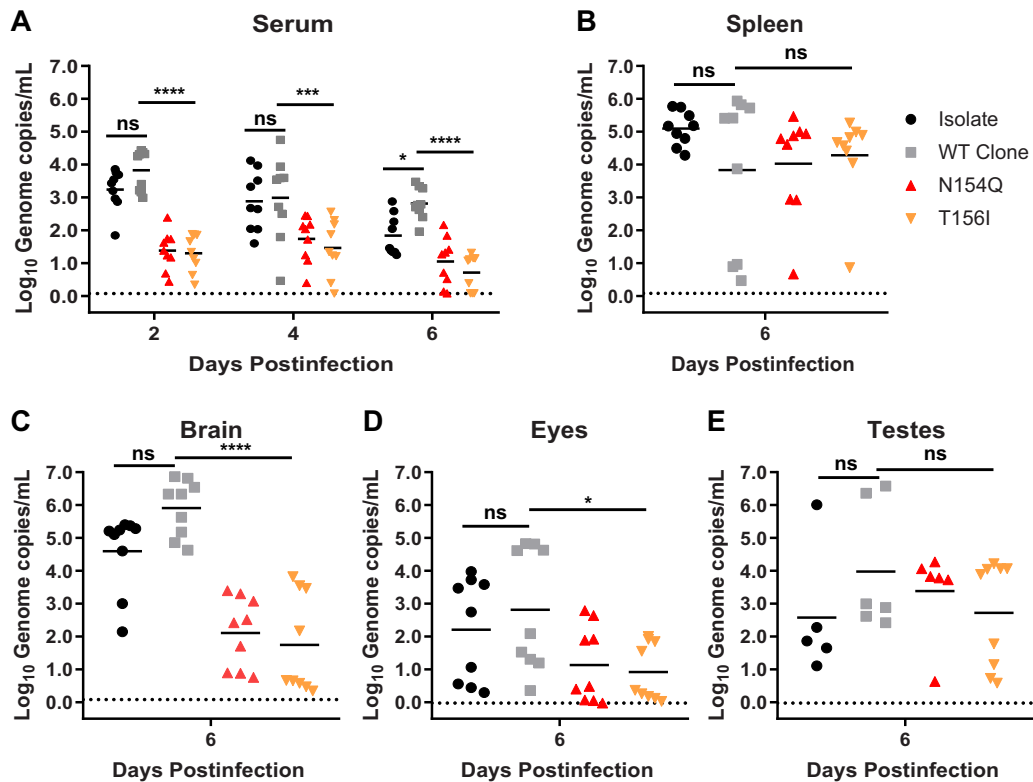
FIG 5 E glycosylation mediates ZIKV PRVABC59 infection in mice. Five- to six-week-old *Ifnar1*$^{-/-}$ mice were inoculated with 1×10^3 FFU of ZIKV strain PRVABC59 isolate, WT clone, N154Q mutant, or T156I mutant by a subcutaneous route in the footpad. (A) Blood was collected at 2, 4, and 6 days after infection, and ZIKV RNA levels in serum were measured by qRT-PCR. (B to E) Mice were euthanized 6 days after infection and perfused, and tissues were harvested. ZIKV RNA in tissues was measured by qRT-PCR. Data are combined from 2 independent experiments. *, $P < 0.05$; ***, $P < 0.001$; ****, $P < 0.0001$; ns, not significant (ANOVA).

serum, as well as in the brain and eyes, indicating that like strain H/PF/2013, ZIKV PRVABC59 infection is mediated by E protein glycosylation *in vivo*. Similar to the results for strain H/PF/2013, glycosylation did not impact ZIKV PRVABC59 viral loads in the spleen or testes. The observation that N154Q and T156I mutants produced very similar viral loads is consistent with a specific role for glycosylation in ZIKV infection, rather than an effect of the Asn residue itself. As we did for the experiments with ZIKV H/PF/2013, we used Sanger sequencing to evaluate viral E sequences from brains harvested 6 days after footpad infection with the ZIKV PRVABC59 N154Q or T156I mutant. In contrast to the results for the H/PF/2013 strain, we found that the mutations were maintained in all 11 brains evaluated (5 infections with the N154Q mutant and 6 with the T156I mutant). These results could indicate that E glycosylation provides a selective advantage for ZIKV H/PF/2013 but not PRVABC59. Alternatively, E glycosylation may be advantageous for both strains, but our stock of H/PF/2013 N154Q virus could contain revertants at a level below the sensitivity of our Sanger sequencing assay, allowing for more rapid selection and amplification *in vivo* than for the PRVABC59 viruses.

H/PF/2013 and PRVABC59 are both Asian-lineage ZIKV strains, closely related to ZIKV strains circulating in the Americas (15, 45). However, the prototype ZIKV strain, MR766, is an African-lineage strain isolated from a sentinel rhesus macaque in 1947 and subsequently maintained by extensive passage in suckling mouse brains (~150 passages) (46). Likely due to this long history, several variants of MR766 have been used by different groups, and nonidentical sequences deposited in NCBI (47, 48). Among the many differences in reference sequences for ZIKV strains named "MR766" is the glycosylation signal at N154, with some sequences encoding an intact glycosylation
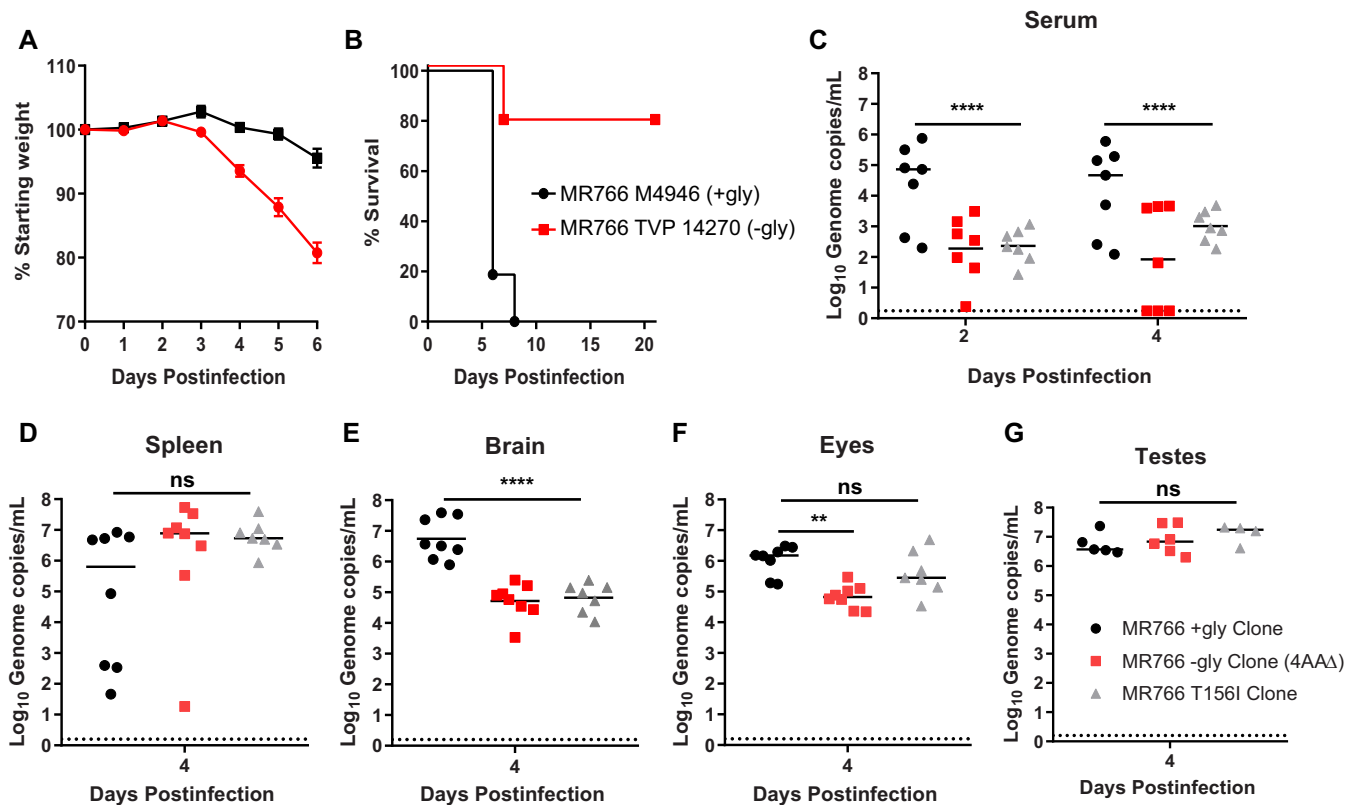
FIG 6 E glycosylation mediates ZIKV MR766 infection in mice. (A and B). Seven- to 10-week-old *Ifnar1*^{−/−} mice were inoculated with 1×10^3 FFU of ZIKV strain MR766 isolates containing the E glycan (+gly) or lacking the E glycan (−gly) by a subcutaneous route in the footpad. Mice were weighed daily, and weights are expressed as percentages of body weight prior to infection and censored once one mouse in a group died. Results shown are the mean values ± SEM of 14 to 16 *Ifnar1*^{−/−} mice per virus. Lethality was monitored for 21 days. (C to G) Five-week-old *Ifnar1*^{−/−} mice were inoculated with 1×10^3 FFU of ZIKV strain MR766 +gly clone, −gly clone 4-amino-acid deletion (4AAΔ), or T156I clone by a subcutaneous route in the footpad. (C) Blood was collected at 2 and 4 days after infection, and ZIKV RNA levels in serum were measured by qRT-PCR. (D to G) Mice were euthanized 4 days after infection and perfused, and tissues were harvested. ZIKV RNA in tissues was measured by qRT-PCR. **, $P < 0.01$; ***, $P < 0.001$; ****, $P < 0.0001$; ns, not significant (ANOVA).

signal (accession number HQ234498.1), some with a T-to-I point mutation that ablates the glycosylation signal (accession number LC002520.1), and others with a 4- to 6-amino-acid deletion that ablates the glycosylation signal (accession numbers DQ859059.1, AY632535.2, and NC_012532.1). To determine whether different MR766 variants exhibited similar levels of virulence *in vivo*, we compared two MR766 isolates obtained from the World Reference Center for Emerging Viruses and Arboviruses: TVP 14270 (SM 150, 7 February 2011) and M4946 (SM 146, 14 October 1952). By Sanger sequencing, we determined that M4946 had an intact glycosylation signal (+gly) at N154, whereas TVP 14270 had a 4-amino-acid deletion ablating this signal (−gly). We infected 7- to 10-week-old *Ifnar1*^{−/−} mice with 1×10^3 FFU of MR766 isolate strains by subcutaneous footpad inoculation. Consistent with a role for E glycosylation in mediating ZIKV virulence, mice infected with M4946 (+gly) lost weight faster and exhibited 100% lethality by 9 dpi, whereas only 20% of mice infected with TVP14270 (−gly) succumbed (Fig. 6A and B). These results are consistent with our previous studies which used MR766 TVP14270 (−gly) (35). We previously reported an infectious clone derived from MR766 TVP 14270 (−gly), as well as mutants that restored the N154 glycosylation signal (+gly) or restored the 4-amino-acid deletion but with the T156I mutation ablating the glycosylation signal (31). To compare the levels of virulence of these isogenic mutants, we infected 5-week-old *Ifnar1*^{−/−} mice with 1×10^3 FFU of MR766 +gly, −gly, and T156I clone viruses via subcutaneous footpad inoculation and measured viral loads in serum at 2 and 4 dpi (Fig. 6C) and in tissues at 4 dpi (Fig. 6D to G). Tissues were harvested at 4 dpi, rather than 6 dpi, because mice succumbed to the +gly virus by 5 dpi, consistent with reports of MR766+gly being more pathogenic than

Asian-lineage strains (49) and MR766 −gly being less pathogenic than H/PF/2013 (35). Similar to the results for ZIKV H/PF/2013 and PRVABC59, we observed lower viral loads at all time points in the serum and in the brain, but not in the testes or spleen, in mice infected with the −gly and T156I viruses than in mice infected with the+gly virus. In the eyes, we found significantly lower viral loads with the −gly virus, but not the T156I virus, compared to the+gly virus. Altogether, our data indicate that ZIKV variants lacking the E protein glycosylation, in both African- and Asian-lineage strains, are attenuated compared to viruses with E protein glycosylation.

Lectins DC-SIGN and DC-SIGNR mediate infection of glycosylated ZIKV. All nonglycosylated ZIKV variants that we tested (6 viruses from strains H/PF/2013, PRVABC59, and MR766) replicated equivalently to their glycosylated counterparts in Vero cells but produced significantly lower levels of viremia in $Ifnar1^{-/-}$ mice. One possible explanation for the *in vivo* attenuation of nonglycosylated viruses could be lower infectivity due to an inability to bind to attachment factors. The lectins DC-SIGN and DC-SIGNR mediate attachment and entry of flaviviruses, including DENV (50–52), WNV (53–55), and JEV (30, 56). DC-SIGN is highly expressed in macrophages and dendritic cells, while DC-SIGNR is expressed on microvascular endothelial cells, especially in the liver sinusoids, lymph nodes, and placental villi (57). To test whether ZIKV E glycosylation facilitates lectin-mediated attachment and infectivity, we used Raji cells and Raji cells expressing DC-SIGN (Raji-DC-SIGN) or DC-SIGNR (Raji-DC-SIGNR) and measured infection by flow cytometry. We confirmed that DC-SIGN and DC-SIGNR were expressed on the surface of the appropriate cell type but not parental Raji cells (Fig. 7A). Cells were infected with ZIKV (strain PRVABC59) WT clone, N154Q mutant, T156I mutant, or UV-inactivated WT clone virus at a multiplicity of infection (MOI) of 5, and intracellular E protein was measured 24 h postinfection (hpi) by flow cytometry (Fig. 7B and C). No E protein signal was detected in cells infected with UV-inactivated virus, confirming that our assay measured viral infection and replication, not residual inoculum. In the absence of exogenous lectin expression, Raji cells were not efficiently infected with ZIKV. However, WT ZIKV, with glycosylated E protein, infected Raji cells expressing exogenous DC-SIGN and, to a greater extent, DC-SIGNR. Infection by nonglycosylated ZIKV (N154Q or T156I) was not augmented by DC-SIGN expression. Unexpectedly, the N154Q mutant was able to infect DC-SIGNR-expressing cells (albeit to a lesser extent than WT virus), while DC-SIGNR did not augment infection by the T156I mutant. Altogether, these data suggest that E glycosylation facilitates ZIKV infection of lectin-expressing leukocytes, which could contribute to lower viremia produced by nonglycosylated ZIKV *in vivo*.

We also used flow cytometry to measure infection of two epithelial cell lines commonly used in ZIKV studies, Vero and A549. Both of these cell lines lack DC-SIGN expression (data not shown), suggesting that entry occurs via different attachment factors. Consistent with the equivalent replication we observed for nonglycosylated ZIKV viruses in Vero cells (Fig. 1C and Fig. 4C), N154Q and T156I mutants exhibited similar infection efficiencies in Vero cells (~75% compared to ~85% of the cell population for WT virus) (Fig. 8A and B). Compared to Vero cells, A549 cells were less permissive to all viruses, but infection was more dependent on E glycosylation (~5% infection with N154Q and T156I viruses compared to ~20% for WT virus) (Fig. 8C and D). The effect of E glycosylation on A549 cell infection also was evident in multistep growth curves, which showed that PRVABC59 N154Q and T156I mutants were attenuated by 10- to 100-fold compared to the WT clone (Fig. 8E). Likewise, replication of the H/PF/2013 N154Q mutant was significantly attenuated in A549 cells compared to that of the WT clone (Fig. 8F). These data suggest that E glycosylation mediates ZIKV infection in A549 cells but is dispensable in Vero cells.

Altogether, our results demonstrate that E glycosylation facilitates ZIKV infection in a tissue-specific manner, which may result from augmented infection of cells expressing certain cell-surface lectins.
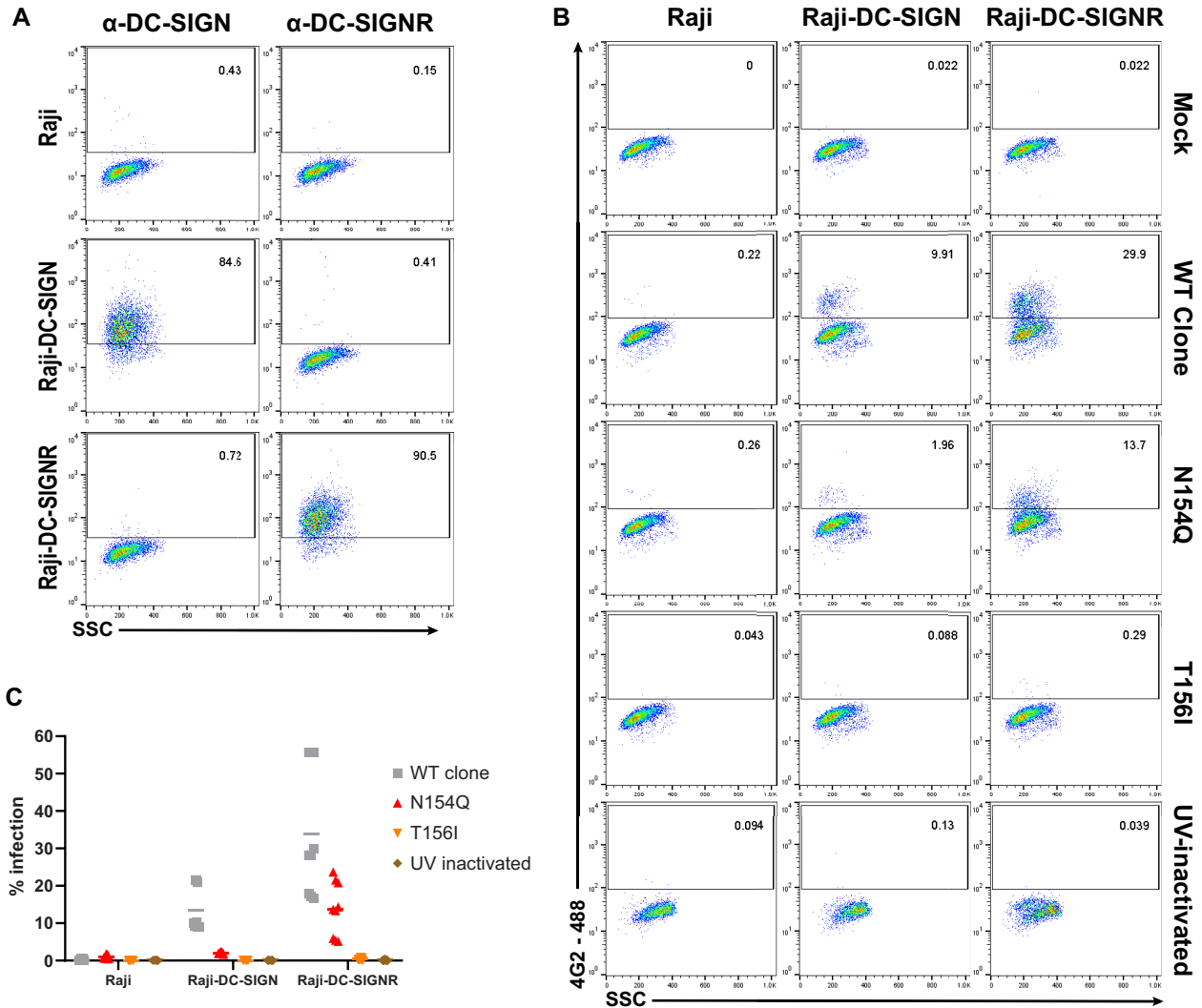
FIG 7 E glycosylation facilitates ZIKV infection of DC-SIGN- and DC-SIGNR-expressing cells. (A) Representative flow cytometry plots of Raji, Raji-DC-SIGN, and Raji-DC-SIGNR cells stained for cell surface expression of DC-SIGN and DC-SIGNR. (B) Representative flow cytometry plots of Raji, Raji-DC-SIGN, and DC-SIGNR cells infected at an MOI of 5 with ZIKV PRVABC59 WT, N154Q, T156I, or UV-inactivated WT virus. Cells were stained at 24 hpi with Alexa Fluor 488-conjugated ZIKV MAb 4G2 to detect intracellular E protein. Values indicate the proportions of cells staining positive. (C) Percentages of infected (E-positive) Raji, Raji-DC-SIGN, or DC-SIGNR cells combined from 3 independent experiments performed in triplicate.

DISCUSSION

The emergence of ZIKV in the Western Hemisphere has been associated with new clinical manifestations, including Guillain-Barre syndrome and congenital Zika syndrome (2). Phylogenetic analyses of ZIKV isolates from past and recent outbreaks have revealed amino acid differences between historic African-lineage strains and the contemporary Asian-lineage strains that are currently circulating in the Western Hemisphere (13–15). Several of these amino acid differences have been implicated in transmission, immune suppression, and enhanced disease. A single amino acid substitution (A188V) in NS1 has been shown to enhance ZIKV antigenemia in mice and infectivity of *Aedes aegypti* mosquitos (16) and also inhibits IFN-β production in cell culture (17). A single amino acid substitution in prM (S139N) has been shown to increase ZIKV replication in human neural progenitor cells and may contribute to a more severe microcephalic phenotype in mice (18), although others found that this mutation is not essential for fetal pathology in a mouse transplacental transmission model (58).

All contemporary Asian-lineage strains possess an intact E glycosylation motif at
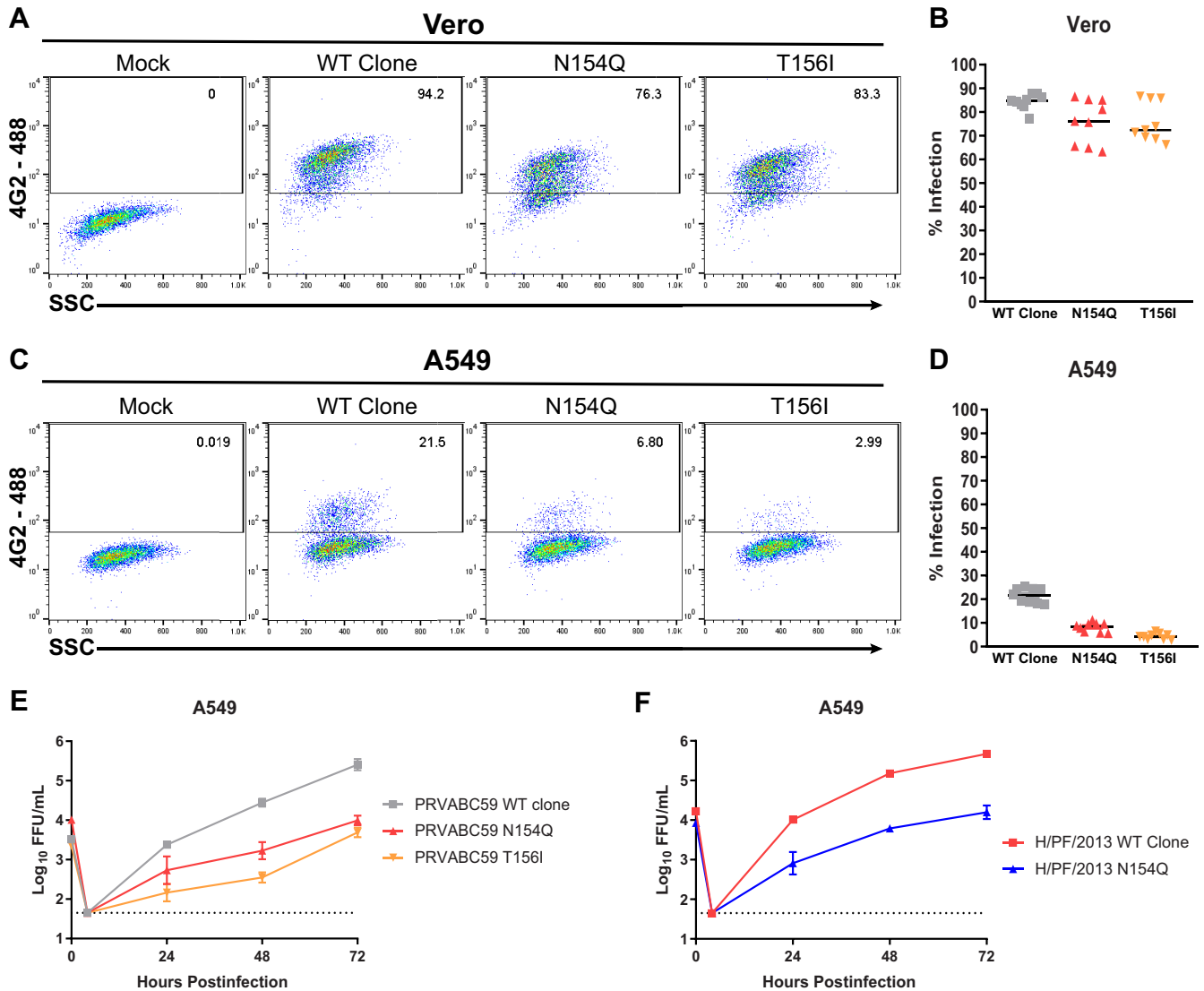
FIG 8 E glycosylation facilitates ZIKV infection of A549 but not Vero cells. (A to D) Vero and A549 cells were infected at an MOI of 5 with ZIKV PRVABC59 WT, N154Q, or T156I clones. Cells were stained at 24 hpi with Alexa Fluor 488-conjugated ZIKV MAb 4G2 to detect intracellular E protein. (A and C) Representative flow cytometry plots of infected Vero or A549 cells. (B and D) Percentages of infected (E positive) Vero or A549 cells combined from 3 independent experiments performed in triplicate. (E and F) A549 cells were infected at an MOI of 0.01 with ZIKV PRVABC59 WT clone, N154Q mutant, or T156I mutant or with ZIKV H/PF/2013 WT clone or N154Q mutant. Viruses in culture supernatants were titrated by focus-forming assay. Data shown are the mean values $\pm$ SEM of 9 samples from 3 independent experiments.

N154Q. In contrast, many historic African-lineage ZIKV strains lack this motif (20, 44), though limited sampling of African ZIKV strains precludes robust conclusions about how common nonglycosylated viruses are in nature. E glycosylation plays a role in attachment and infectivity for DENV (50), WNV (53, 55, 59), and JEV (56) and has been associated with enhanced mosquito transmission and/or increased virulence and neuroinvasion in vertebrates for other flaviviruses (21–30). We investigated the role of the ZIKV E glycosylation in tissue tropism and pathogenesis in an immunocompromised mouse model. Our results indicate that both Asian- and African-lineage ZIKV strains lacking E glycosylation sustained lower tissue viral loads than did WT virus. These results are consistent with other reports of a role for E glycosylation in mediating ZIKV virulence. Annamalai et al. showed that ZIKV strain MR766 lacking E glycosylation due to a 4-amino-acid deletion or an N154A substitution produced lower viral loads in serum and brains of A129 mice than did glycosylated virus (37). Similarly, Fontes-Garfias et al. showed that a Cambodian ZIKV strain lacking E glycosylation due to an N154Q

substitution resulted in decreased viral loads in serum of A129 mice compared to the WT glycosylated virus (42). Notably, even though we found that ZIKV lacking E glycosylation resulted in lower viral loads than did glycosylated virus in the serum, eyes, and brains, we observed similar viral loads in the spleen and testes, consistent with a previous report that glycosylated and nonglycosylated ZIKV strain MR766 sustained similar viral loads in the spleen and liver (37). Likewise, a nonglycosylated mutant of Tembusu virus produced equivalent viral loads in the spleens of infected ducks, despite reduced viral loads in other tissues (26). Furthermore, our observation that the ZIKV H/PF/2013 N154Q mutation was maintained upon intracranial inoculation but selected against after subcutaneous inoculation suggests that glycosylation provides a selective advantage to ZIKV in peripheral tissues but not within the brain. Altogether, these observations suggest that E glycosylation facilitates infection of ZIKV, and perhaps other flaviviruses, in a tissue or cell type-specific manner.

E glycosylation likely facilitates attachment to and infection of lectin-expressing cells, including $CD14^+$ monocyte cells that are targets of ZIKV in humans (60–63). DC-SIGN and DC-SIGNR are among several attachment factors described for flaviviruses, such as DENV (50, 51, 64), JEV (30, 56), and WNV (53, 54, 59), as well as for ZIKV (65–67), though it is less clear which lectins or other attachment factors actually mediate ZIKV infection in mice or humans (68–70). Though mice do not have clear DC-SIGN or DC-SIGNR orthologs, they have eight DC-SIGN homologs clustered within the same genomic region (60). According to their glycan specificity, murine SIGNR1 and SIGNR3 are the closest candidates to fulfill DC-SIGN function in mice, but their ability to facilitate flavivirus infection is unclear. Unexpectedly, we found that DC-SIGNR was able to augment infection by the N154Q mutant, even in the absence of E glycosylation, which was unlike the T156I mutant. The different infection efficiencies of the two nonglycosylated mutants on Raji-DC-SIGNR cells could result from less efficient maturation of N154Q virions than of T156I virions; in this case, glycosylated prM on immature N154Q virions may partially complement the loss of E glycosylation (67). Cleavage of prM is required to produce mature infectious flavivirus virions because interactions between prM and E prevent the conformational changes required to drive pH-dependent membrane fusion, but partially mature virions also can be infectious (71). The cleaved portion of prM is glycosylated, and uncleaved prM on partially mature virions can facilitate attachment and entry in a DC-SIGNR-dependent manner (54, 67). Alternatively, the difference in infection efficiencies in DC-SIGNR cells could indicate a specific role for Gln 154 or Thr 156 independent of glycosylation, perhaps through modulation of the glycan loop and resulting effects on attachment and fusion (67, 72). Overall, our findings demonstrate a role for E glycosylation in ZIKV pathogenesis, possibly by facilitating attachment to and infection of lectin-expressing leukocytes.

MATERIALS AND METHODS

Cells and viruses. Vero and A549 cells were maintained in Dulbecco's modified Eagle medium (DMEM) containing 10% heat-inactivated fetal bovine serum (FBS) and L-glutamine at 37°C with 5% CO_2. Raji, Raji-DC-SIGN, and Raji-DC-SIGNR cells were obtained from Theodore Pierson (NIH) (54). Raji cells were maintained in RPMI 1640 medium supplemented with 10% FBS and penicillin-streptomycin. ZIKV strains H/PF/2013 and PRVABC59 were provided by the U.S. Centers for Disease Control and Prevention (41, 43). The ZIKV MR766 strains were obtained from the World Reference Center for Emerging Viruses and Arboviruses (46–48). The DENV-3 WHO reference strain (CH54389) was obtained from Aravinda de Silva (UNC) (73). Virus stocks were grown in Vero (African green monkey kidney epithelial) cells. Virus stocks were titrated on Vero cells by focus-forming assay (FFA) (74). For multistep growth analysis, cells were infected at an MOI of 0.01 and incubated at 37°C with 5% CO_2. Samples of infected cell culture supernatant were collected at 4, 24, 48, and 72 hpi and stored at −80°C for virus titration. Virus quantification was performed by FFA on Vero cells. Duplicate serial 10-fold dilutions of virus in viral growth medium (DMEM containing 2% FBS and 20 mM HEPES) were applied to Vero cells in 96-well plates and incubated at 37°C with 5% CO_2 for 1 h. Cells were then overlaid with 1% methylcellulose in minimum essential medium Eagle (MEM). Infected cell foci were detected 42 to 46 hpi. Following fixation with 2% paraformaldehyde for 1 h at room temperature, plates were incubated with 500 ng/ml of flavivirus cross-reactive mouse MAb E60 (75) for 2 h at room temperature or overnight at 4°C. After incubation at room temperate for 2 h with a 1:5,000 dilution of horseradish peroxidase (HRP)-conjugated goat anti-mouse IgG (Sigma), foci were detected by the addition of TrueBlue substrate (KPL). Foci were quantified with a CTL Immunospot instrument. To prepare UV-inactivated virus, 20 ml of PRVABC59 WT

clone virus (1×10^5 FFU/ml) was placed in a petri dish and exposed to UV light at 0.9 J/cm² for 10 min in an HL-2000 HybriLinker (UVP Laboratory Products); inactivation was confirmed by FFA.

ZIKV infectious clone design and mutagenesis. We used a quadripartite unidirectional molecular clone strategy, as previously described (31), to generate a new infectious clone of ZIKV strain PRVABC59. Due to the high sequence similarity between H/PF/2013 and PRVABC59, we were able to use the same naturally occurring class IIG nonpalindromic restriction endonuclease sites within the full-length genome as previously described for ZIKV strain H/PF/2013 (31). NotI and EcoRV restriction endonuclease sites, followed by a T7 promoter sequence for *in vitro* transcription, were added to the immediate 5′ end of the genome. A hepatitis delta virus (HDV) ribozyme sequence, to generate an intact 3′ untranslated region (UTR), followed by an SmaI restriction endonuclease site, was added directly after the last nucleotide of the genome. The four subgenomic fragments were synthesized into the pUC-57 vector (BioBasic) and amplified in One Shot TOP10 chemically competent *Escherichia coli* cells (Thermo) grown on LB plates with carbenicillin at 37°C for ~16 h. Individual colonies were picked, grown in selective LB, purified (Qiagen mini-spin kit), and sequenced. The resulting purified plasmids were digested, ligated, *in vitro* transcribed, and electroporated into Vero cells as previously described (76). Supernatants from electroporated Vero cells were harvested after 6 to 7 days and passaged once on Vero cells to generate virus stocks. Virus stocks were titrated by FFA on Vero cells. Site-directed mutagenesis was used to introduce a single amino acid substitution (N154Q or T156I) in the envelope protein to ablate the glycosylation motif. Restriction enzymes and the Phusion high-fidelity PCR kit were obtained from New England BioLabs. The SuperScript III first-strand synthesis kit was obtained from Invitrogen. Oligonucleotide primers and probes for DNA amplification, qRT-PCR, and sequencing were obtained from Sigma and IDT. The mMachine T7 ultra transcription kit was obtained from Ambion.

Glycosylation assays. MAbs E60, 1M7, and 4G2 all recognize the conserved flavivirus fusion loop and were produced by the UNC Protein Expression and Purification Core Facility (75, 77, 78). E protein was immunoprecipitated from infected Vero cell lysates using MAb 1M7 (1 μg) and magnetic protein A/G beads (Pierce). Immunoprecipitated E protein was digested with peptide N-glycosidase F (PNGaseF; New England BioLabs) according to the manufacturer's protocol with a minor modification. Instead of denaturation in the provided glycoprotein denaturation buffer containing dithiothreitol, immunoprecipitates were denatured in 0.5% SDS, because the epitope recognized by MAb 4G2 is reduction sensitive (79). PNGaseF digestions were separated by SDS-PAGE (7.5% precast polyacrylamide gels; Bio-Rad) under nonreducing conditions and analyzed by Western or lectin blotting. Proteins were transferred to a nitrocellulose membrane using a Trans-Blot Turbo transfer system (Bio-Rad). In Western blots, E protein was detected using MAb 4G2 as a primary antibody and HRP-conjugated goat anti-mouse IgG as a secondary antibody. For lectin blots, glycosylated E was detected with the biotinylated lectin concanavalin A (ConA; Vector Laboratories), followed by HRP-conjugated streptavidin. Pierce ECL Western blotting substrate was used to detect HRP (Thermo). Western and lectin blots were imaged on a ChemiDoc XRS+ system (Bio-Rad).

Mouse experiments. Animal husbandry and experiments were performed under the approval of the University of North Carolina at Chapel Hill Institutional Animal Care and Use Committee. Five- to 6-week-old or 7- to 10-week-old male and female wild-type or *Ifnar1*$^{-/-}$ mice on a C57BL/6 background were used. Mice were inoculated with 1×10^3 FFU of ZIKV in a volume of 50 μl subcutaneously (footpad) or 25 μl intracranially. Survival and weight loss were monitored for 14 or 21 days. Animals that lost >30% of their starting weight or that became moribund were euthanized.

Measurement of viral loads. ZIKV-infected mice were sacrificed at 4 or 6 dpi and perfused with 20 ml of phosphate-buffered saline (PBS). Spleen, kidney, testes, brain, and eyes were harvested and homogenized with zirconia beads (BioSpec) in a MagNA Lyser instrument (Roche Life Science) in 500 μl (eyes) or 1 ml (all other tissues) of buffer RLT (Qiagen). Blood was collected at 2 and 4 dpi by submandibular bleeds with a 5-mm Goldenrod lancet and by cardiac puncture at 6 dpi. Blood was collected in serum separator tubes (BD), and serum was separated by centrifugation at 8,000 rpm for 5 min. Tissues and serum from infected animals were stored at −80°C until RNA isolation. RNA was extracted with the RNeasy minikit (tissues) or viral RNA minikit (serum) (Qiagen). ZIKV RNA levels were determined by TaqMan one-step qRT-PCR on a CFX96 Touch real-time PCR detection system (Bio-Rad) using standard cycling conditions. Viral burdens are expressed on a Log_{10} scale as either viral RNA equivalents per ml after comparison with a standard curve produced using serial 10-fold dilutions of RNA extracted from a ZIKV stock or genome copies per ml after comparison with a standard curve produced using serial 100-fold dilutions of ZIKV A plasmid. The following previously published primer set was used to detect ZIKV H/PF/2013 and PRVABC59 RNA: forward, CCGCTGCCCAACACAAG; reverse, CCACTAACGT TCTTTTGCAGACAT; and probe, 56-FAM/AGCCTACCT/ZEN/TGACAAGCAATCAGACACTCAA/3IABkFQ (Integrated DNA Technologies) (80). ZIKV MR766 RNA was detected using the following primers: forward, GGGCGTGTCATATTCCTTGT; reverse, TCCATCTGTCCCTGCATACT; and probe, 56-FAM/AGCCTACCT/ZEN/TGACAAGCAATCAGACACTCAA/3IABkFQ (Integrated DNA Technologies).

Flow cytometry. Cells (2×10^4) were infected with ZIKV at an MOI of 5 for 1 h at 37°C in RPMI 1640 or DMEM supplemented with 2% FBS. The cells were subsequently washed with fluorescence-activated cell sorting (FACS) buffer (PBS with 1% FBS) to remove excess virus and incubated at 37°C for 24 h. Following incubation, cells were washed with FACS buffer and fixed by adding 100 μl of 1% paraformaldehyde (PFA) and incubating at 4°C for 10 min. Cells were subsequently washed with permeabilization buffer (PBS with 0.1% bovine serum albumin [BSA] and 0.1% saponin). The permeabilized cells were stained for ZIKV E protein using MAb 4G2 conjugated to Alexa Fluor 488, diluted 1:200, for 30 min at 4°C. For extracellular staining, cell surface DC-SIGN and DC-SIGNR were stained using MAb 9E9A8 for DC-SIGN (BioLegend) and MAB162 for DC-SIGNR (R&D Systems) at 4°C for 30 min. After washing with FACS buffer,

cells were fixed and permeabilized as described above. The permeabilized cells were stained with secondary anti-mouse IgG–peridinin chlorophyll protein (PerCP), diluted 1:100. The stained cells were subsequently washed with FACS buffer and analyzed using a Guava EasyCyte HT flow cytometer (Millipore).

Data analysis. All data were analyzed with GraphPad Prism software. Flow cytometry data were analyzed with FlowJo version 10 software. Kaplan-Meier survival curves were analyzed by the log-rank test, and weight losses were compared using two-way analysis of variance (ANOVA). For viral burden analysis, the log-transformed titers were analyzed by ANOVA or 2-tailed t test. P values of <0.05 indicated statistically significant differences.

REFERENCES

1. Petersen LR, Jamieson DJ, Powers AM, Honein MA. 2016. Zika virus. N Engl J Med 374:1552–1563. https://doi.org/10.1056/NEJMra1602113.
2. Pierson TC, Diamond MS. 2018. The emergence of Zika virus and its new clinical syndromes. Nature 560:573–581. https://doi.org/10.1038/s41586-018-0446-y.
3. Oehler E, Watrin L, Larre P, Leparc-Goffart I, Lastere S, Valour F, Baudouin L, Mallet H, Musso D, Ghawche F. 2014. Zika virus infection complicated by Guillain-Barre syndrome—case report, French Polynesia, December 2013. Euro Surveill 19:20720.
4. Munoz LS, Parra B, Pardo CA, Neuroviruses Emerging in the Americas Study. 2017. Neurological implications of Zika virus infection in adults. J Infect Dis 216:S897–S905. https://doi.org/10.1093/infdis/jix511.
5. Zanluca C, Melo VC, Mosimann AL, Santos GI, Santos CN, Luz K. 2015. First report of autochthonous transmission of Zika virus in Brazil. Mem Inst Oswaldo Cruz 110:569–572. https://doi.org/10.1590/0074-02760150192.
6. Campos GS, Bandeira AC, Sardi SI. 2015. Zika virus outbreak, Bahia, Brazil. Emerg Infect Dis 21:1885–1886. https://doi.org/10.3201/eid2110.150847.
7. Metsky HC, Matranga CB, Wohl S, Schaffner SF, Freije CA, Winnicki SM, West K, Qu J, Baniecki ML, Gladden-Young A, Lin AE, Tomkins-Tinch CH, Ye SH, Park DJ, Luo CY, Barnes KG, Shah RR, Chak B, Barbosa-Lima G, Delatorre E, Vieira YR, Paul LM, Tan AL, Barcellona CM, Porcelli MC, Vasquez C, Cannons AC, Cone MR, Hogan KN, Kopp EW, Anzinger JJ, Garcia KF, Parham LA, Ramírez RMG, Montoya MCM, Rojas DP, Brown CM, Hennigan S, Sabina B, Scotland S, Gangavarapu K, Grubaugh ND, Oliveira G, Robles-Sikisaka R, Rambaut A, Gehrke L, Smole S, Halloran ME, Villar L, Mattar S, et al. 2017. Zika virus evolution and spread in the Americas. Nature 546:411–415. https://doi.org/10.1038/nature22402.
8. Faria NR, Quick J, Claro IM, Thézé J, de Jesus JG, Giovanetti M, Kraemer MUG, Hill SC, Black A, da Costa AC, Franco LC, Silva SP, Wu C-H, Raghwani J, Cauchemez S, Du Plessis L, Verotti MP, de Oliveira WK, Carmo EH, Coelho GE, Santelli ACFS, Vinhal LC, Henriques CM, Simpson JT, Loose M, Andersen KG, Grubaugh ND, Somasekar S, Chiu CY, Muñoz-Medina JE, Gonzalez-Bonilla CR, Arias CF, Lewis-Ximenez LL, Baylis SA, Chieppe AO, Aguiar SF, Fernandes CA, Lemos PS, Nascimento BLS, Monteiro HAO, Siqueira IC, de Queiroz MG, de Souza TR, Bezerra JF, Lemos MR, Pereira GF, Loudal D, Moura LC, Dhalia R, França RF, et al. 2017. Establishment and cryptic transmission of Zika virus in Brazil and the Americas. Nature 546:406–410. https://doi.org/10.1038/nature22401.
9. Coyne CB, Lazear HM. 2016. Zika virus—reigniting the TORCH. Nat Rev Microbiol 14:707–715. https://doi.org/10.1038/nrmicro.2016.125.
10. Brady OJ, Osgood-Zimmerman A, Kassebaum NJ, Ray SE, de Araujo VEM, da Nobrega AA, Frutuoso LCV, Lecca RCR, Stevens A, Zoca de Oliveira B, de Lima JM, Jr, Bogoch II, Mayaud P, Jaenisch T, Mokdad AH, Murray CJL, Hay SI, Reiner RC, Jr, Marinho F. 2019. The association between Zika virus infection and microcephaly in Brazil 2015–2017: an observational analysis of over 4 million births. PLoS Med 16:e1002755. https://doi.org/10.1371/journal.pmed.1002755.
11. Liu ZY, Shi WF, Qin CF. 2019. The evolution of Zika virus from Asia to the Americas. Nat Rev Microbiol 17:131–139. https://doi.org/10.1038/s41579-018-0134-9.
12. Grubaugh ND, Ishtiaq F, Setoh YX, Ko AI. 27 February 2019. Misperceived risks of Zika-related microcephaly in India. Trends Microbiol https://doi.org/10.1016/j.tim.2019.02.004.
13. Zhu Z, Chan JF, Tee KM, Choi GK, Lau SK, Woo PC, Tse H, Yuen KY. 2016. Comparative genomic analysis of pre-epidemic and epidemic Zika virus strains for virological factors potentially associated with the rapidly expanding epidemic. Emerg Microbes Infect 5:e22. https://doi.org/10.1038/emi.2016.48.
14. Wang L, Valderramos SG, Wu A, Ouyang S, Li C, Brasil P, Bonaldo M, Coates T, Nielsen-Saines K, Jiang T, Aliyari R, Cheng G. 2016. From mosquitos to humans: genetic evolution of Zika virus. Cell Host Microbe 19:561–565. https://doi.org/10.1016/j.chom.2016.04.006.
15. Pettersson JH, Eldholm V, Seligman SJ, Lundkvist A, Falconar AK, Gaunt MW, Musso D, Nougairede A, Charrel R, Gould EA, de Lamballerie X. 2016. How did Zika virus emerge in the Pacific Islands and Latin America? mBio 7:e01239-16. https://doi.org/10.1128/mBio.01239-16.
16. Liu Y, Liu J, Du S, Shan C, Nie K, Zhang R, Li XF, Zhang R, Wang T, Qin CF, Wang P, Shi PY, Cheng G. 2017. Evolutionary enhancement of Zika virus infectivity in Aedes aegypti mosquitoes. Nature 545:482–486. https://doi.org/10.1038/nature22365.
17. Xia H, Luo H, Shan C, Muruato AE, Nunes BTD, Medeiros DBA, Zou J, Xie X, Giraldo MI, Vasconcelos PFC, Weaver SC, Wang T, Rajsbaum R, Shi PY. 2018. An evolutionary NS1 mutation enhances Zika virus evasion of host interferon induction. Nat Commun 9:414. https://doi.org/10.1038/s41467-017-02816-2.
18. Yuan L, Huang XY, Liu ZY, Zhang F, Zhu XL, Yu JY, Ji X, Xu YP, Li G, Li C, Wang HJ, Deng YQ, Wu M, Cheng ML, Ye Q, Xie DY, Li XF, Wang X, Shi W, Hu B, Shi PY, Xu Z, Qin CF. 2017. A single mutation in the prM protein of Zika virus contributes to fetal microcephaly. Science 358:933–936. https://doi.org/10.1126/science.aam7120.
19. Haddow AD, Schuh AJ, Yasuda CY, Kasper MR, Heang V, Huy R, Guzman H, Tesh RB, Weaver SC. 2012. Genetic characterization of Zika virus strains: geographic expansion of the Asian lineage. PLoS Negl Trop Dis 6:e1477. https://doi.org/10.1371/journal.pntd.0001477.
20. Faye O, Freire CC, Iamarino A, Faye O, de Oliveira JV, Diallo M, Zanotto PM, Sall AA. 2014. Molecular evolution of Zika virus during its emergence in the 20(th) century. PLoS Negl Trop Dis 8:e2636. https://doi.org/10.1371/journal.pntd.0002636.
21. Yoshii K, Yanagihara N, Ishizuka M, Sakai M, Kariwa H. 2013. N-linked glycan in tick-borne encephalitis virus envelope protein affects viral secretion in mammalian cells, but not in tick cells. J Gen Virol 94:2249–2258. https://doi.org/10.1099/vir.0.055269-0.
22. Prow NA, May FJ, Westlake DJ, Hurrelbrink RJ, Biron RM, Leung JY, McMinn PC, Clark DC, Mackenzie JS, Lobigs M, Khromykh AA, Hall RA. 2011. Determinants of attenuation in the envelope protein of the flavivirus Alfuy. J Gen Virol 92:2286–2296. https://doi.org/10.1099/vir.0.034793-0.
23. Beasley DW, Whiteman MC, Zhang S, Huang CY, Schneider BS, Smith DR, Gromowski GD, Higgs S, Kinney RM, Barrett AD. 2005. Envelope protein glycosylation status influences mouse neuroinvasion phenotype of genetic lineage 1 West Nile virus strains. J Virol 79:8339–8347. https://doi.org/10.1128/JVI.79.13.8339-8347.2005.

24. Shirato K, Miyoshi H, Goto A, Ako Y, Ueki T, Kariwa H, Takashima I. 2004. Viral envelope protein glycosylation is a molecular determinant of the neuroinvasiveness of the New York strain of West Nile virus. J Gen Virol 85:3637–3645. https://doi.org/10.1099/vir.0.80247-0.

25. Jiang WR, Lowe A, Higgs S, Reid H, Gould EA. 1993. Single amino acid codon changes detected in louping ill virus antibody-resistant mutants with reduced neurovirulence. J Gen Virol 74:931–935. https://doi.org/10.1099/0022-1317-74-5-931.

26. Yan D, Shi Y, Wang H, Li G, Li X, Wang B, Su X, Wang J, Teng Q, Yang J, Chen H, Liu Q, Ma W, Li Z. 2018. A single mutation at position 156 in the envelope protein of Tembusu virus is responsible for virus tissue tropism and transmissibility in ducks. J Virol 92:e00427-18. https://doi.org/10.1128/JVI.00427-18.

27. Moudy RM, Zhang B, Shi PY, Kramer LD. 2009. West Nile virus envelope protein glycosylation is required for efficient viral transmission by Culex vectors. Virology 387:222–228. https://doi.org/10.1016/j.virol.2009.01.038.

28. Murata R, Eshita Y, Maeda A, Maeda J, Akita S, Tanaka T, Yoshii K, Kariwa H, Umemura T, Takashima I. 2010. Glycosylation of the West Nile Virus envelope protein increases in vivo and in vitro viral multiplication in birds. Am J Trop Med Hyg 82:696–704. https://doi.org/10.4269/ajtmh.2010.09-0262.

29. Wen D, Li S, Dong F, Zhang Y, Lin Y, Wang J, Zou Z, Zheng A. 2018. N-glycosylation of viral E protein is the determinant for vector midgut invasion by flaviviruses. mBio 9:e00046-18. https://doi.org/10.1128/mBio.00046-18.

30. Liang JJ, Chou MW, Lin YL. 2018. DC-SIGN binding contributed by an extra N-linked glycosylation on Japanese encephalitis virus envelope protein reduces the ability of viral brain invasion. Front Cell Infect Microbiol 8:239. https://doi.org/10.3389/fcimb.2018.00239.

31. Widman DG, Young E, Yount BL, Plante KS, Gallichotte EN, Carbaugh DL, Peck KM, Plante J, Swanstrom J, Heise MT, Lazear HM, Baric RS. 2017. A reverse genetics platform that spans the Zika virus family tree. mBio 8:e02014-16. https://doi.org/10.1128/mBio.02014-16.

32. Hacker K, White L, de Silva AM. 2009. N-linked glycans on dengue viruses grown in mammalian and insect cells. J Gen Virol 90:2097–2106. https://doi.org/10.1099/vir.0.012120-0.

33. Kumar A, Hou S, Airo AM, Limonta D, Mancinelli V, Branton W, Power C, Hobman TC. 2016. Zika virus inhibits type-I interferon production and downstream signaling. EMBO Rep 17:1766–1775. https://doi.org/10.15252/embr.201642627.

34. Grant A, Ponia SS, Tripathi S, Balasubramaniam V, Miorin L, Sourisseau M, Schwarz MC, Sánchez-Seco MP, Evans MJ, Best SM, García-Sastre A. 2016. Zika virus targets human STAT2 to inhibit type i interferon signaling. Cell Host Microbe 19:882–890. https://doi.org/10.1016/j.chom.2016.05.009.

35. Lazear HM, Govero J, Smith AM, Platt DJ, Fernandez E, Miner JJ, Diamond MS. 2016. A mouse model of Zika virus pathogenesis. Cell Host Microbe 19:720–730. https://doi.org/10.1016/j.chom.2016.03.010.

36. Rossi SL, Tesh RB, Azar SR, Muruato AE, Hanley KA, Auguste AJ, Langsjoen RM, Paessler S, Vasilakis N, Weaver SC. 2016. Characterization of a novel murine model to study Zika virus. Am J Trop Med Hyg 94:1362–1369. https://doi.org/10.4269/ajtmh.16-0111.

37. Annamalai AS, Pattnaik A, Sahoo BR, Muthukrishnan E, Natarajan SK, Steffen D, Vu HLX, Delhon G, Osorio FA, Petro TM, Xiang SH, Pattnaik AK. 2017. Zika virus encoding non-glycosylated envelope protein is attenuated and defective in neuroinvasion. J Virol 91:e01348-17. https://doi.org/10.1128/JVI.01348-17.

38. Musso D, Bossin H, Mallet HP, Besnard M, Broult J, Baudouin L, Levi JE, Sabino EC, Ghawche F, Lanteri MC, Baud D. 2018. Zika virus in French Polynesia 2013-14: anatomy of a completed outbreak. Lancet Infect Dis 18:e172–e182. https://doi.org/10.1016/S1473-3099(17)30446-2.

39. Cauchemez S, Besnard M, Bompard P, Dub T, Guillemette-Artur P, Eyrolle-Guignot D, Salje H, Van Kerkhove MD, Abadie V, Garel C, Fontanet A, Mallet HP. 2016. Association between Zika virus and microcephaly in French Polynesia, 2013-15: a retrospective study. Lancet 387:2125–2132. https://doi.org/10.1016/S0140-6736(16)00651-6.

40. Cao-Lormeau VM, Roche C, Teissier A, Robin E, Berry AL, Mallet HP, Sall AA, Musso D. 2014. Zika virus, French polynesia, South Pacific, 2013. Emerg Infect Dis 20:1085–1086. https://doi.org/10.3201/eid2006.140138.

41. Baronti C, Piorkowski G, Charrel RN, Boubis L, Leparc-Goffart I, de Lamballerie X. 2014. Complete coding sequence of Zika virus from a French Polynesia outbreak in 2013. Genome Announc 2:e00500-14. https://doi.org/10.1128/genomeA.00500-14.

42. Fontes-Garfias CR, Shan C, Luo H, Muruato AE, Medeiros DBA, Mays E, Xie

X, Zou J, Roundy CM, Wakamiya M, Rossi SL, Wang T, Weaver SC, Shi PY. 2017. Functional analysis of glycosylation of Zika virus envelope protein. Cell Rep 21:1180–1190. https://doi.org/10.1016/j.celrep.2017.10.016.

43. Lanciotti RS, Lambert AJ, Holodniy M, Saavedra S, Signor LC. 2016. Phylogeny of Zika virus in Western Hemisphere, 2015. Emerg Infect Dis 22:933–935. https://doi.org/10.3201/eid2205.160065.

44. Berthet N, Nakoune E, Kamgang B, Selekon B, Descorps-Declere S, Gessain A, Manuguerra JC, Kazanji M. 2014. Molecular characterization of three Zika flaviviruses obtained from sylvatic mosquitoes in the Central African Republic. Vector Borne Zoonotic Dis 14:862–865. https://doi.org/10.1089/vbz.2014.1607.

45. Faria NR, Azevedo RDSDS, Kraemer MUG, Souza R, Cunha MS, Hill SC, Theze J, Bonsall MB, Bowden TA, Rissanen I, Rocco IM, Nogueira JS, Maeda AY, Vasami FGDS, Macedo FLL, Suzuki A, Rodrigues SG, Cruz ACR, Nunes BT, Medeiros DBA, Rodrigues DSG, Nunes Queiroz AL, da Silva EVP, Henriques DF, Travassos da Rosa ES, de Oliveira CS, Martins LC, Vasconcelos HB, Casseb LMN, Simith DB, Messina JP, Abade L, Lourenco J, Alcantara LCJ, de Lima MM, Giovanetti M, Hay SI, de Oliveira RS, Lemos PDS, de Oliveira LF, de Lima CPS, da Silva SP, de Vasconcelos JM, Franco L, Cardoso JF, Vianez-Junior JLDSG, Mir D, Bello G, Delatorre E, Khan K, et al. 2016. Zika virus in the Americas: early epidemiological and genetic findings. Science 352:345–349. https://doi.org/10.1126/science.aaf5036.

46. Dick GW, Kitchen SF, Haddow AJ. 1952. Zika virus. I. Isolations and serological specificity. Trans R Soc Trop Med Hyg 46:509–520. https://doi.org/10.1016/0035-9203(52)90042-4.

47. Ladner JT, Wiley MR, Prieto K, Yasuda CY, Nagle E, Kasper MR, Reyes D, Vasilakis N, Heang V, Weaver SC, Haddow A, Tesh RB, Sovann L, Palacios G. 2016. Complete genome sequences of five Zika virus isolates. Genome Announc 4:e00377-16. https://doi.org/10.1128/genomeA.00377-16.

48. Yun SI, Song BH, Frank JC, Julander JG, Polejaeva IA, Davies CJ, White KL, Lee YM. 2016. Complete genome sequences of three historically important, spatiotemporally distinct, and genetically divergent strains of Zika virus: MR-766, P6-740, and PRVABC-59. Genome Announc 4:e00800-16. https://doi.org/10.1128/genomeA.00800-16.

49. Tripathi S, Balasubramaniam VRMT, Brown JA, Mena I, Grant A, Bardina SV, Maringer K, Schwarz MC, Maestre AM, Sourisseau M, Albrecht RA, Krammer F, Evans MJ, Fernandez-Sesma A, Lim JK, García-Sastre A. 2017. A novel Zika virus mouse model reveals strain specific differences in virus pathogenesis and host inflammatory immune responses. PLoS Pathog 13:e1006258. https://doi.org/10.1371/journal.ppat.1006258.

50. Mondotte JA, Lozach PY, Amara A, Gamarnik AV. 2007. Essential role of dengue virus envelope protein N glycosylation at asparagine-67 during viral propagation. J Virol 81:7136–7148. https://doi.org/10.1128/JVI.00116-07.

51. Tassaneetrithep B, Burgess TH, Granelli-Piperno A, Trumpfheller C, Finke J, Sun W, Eller MA, Pattanapanyasat K, Sarasombath S, Birx DL, Steinman RM, Schlesinger S, Marovich MA. 2003. DC-SIGN (CD209) mediates dengue virus infection of human dendritic cells. J Exp Med 197:823–829. https://doi.org/10.1084/jem.20021840.

52. Rouvinski A, Guardado-Calvo P, Barba-Spaeth G, Duquerroy S, Vaney M-C, Kikuti CM, Navarro Sanchez ME, Dejnirattisai W, Wongwiwat W, Haouz A, Girard-Blanc C, Petres S, Shepard WE, Desprès P, Arenzana-Seisdedos F, Dussart P, Mongkolsapaya J, Screaton GR, Rey FA. 2015. Recognition determinants of broadly neutralizing human antibodies against dengue viruses. Nature 520:109–113. https://doi.org/10.1038/nature14130.

53. Martina BE, Koraka P, van den Doel P, Rimmelzwaan GF, Haagmans BL, Osterhaus AD. 2008. DC-SIGN enhances infection of cells with glycosylated West Nile virus in vitro and virus replication in human dendritic cells induces production of IFN-alpha and TNF-alpha. Virus Res 135:64–71. https://doi.org/10.1016/j.virusres.2008.02.008.

54. Davis CW, Nguyen HY, Hanna SL, Sanchez MD, Doms RW, Pierson TC. 2006. West Nile virus discriminates between DC-SIGN and DC-SIGNR for cellular attachment and infection. J Virol 80:1290–1301. https://doi.org/10.1128/JVI.80.3.1290-1301.2006.

55. Davis CW, Mattei LM, Nguyen HY, Ansarah-Sobrinho C, Doms RW, Pierson TC. 2006. The location of asparagine-linked glycans on West Nile virions controls their interactions with CD209 (dendritic cell-specific ICAM-3 grabbing nonintegrin). J Biol Chem 281:37183–37194. https://doi.org/10.1074/jbc.M605429200.

56. Wang P, Hu K, Luo S, Zhang M, Deng X, Li C, Jin W, Hu B, He S, Li M, Du T, Xiao G, Zhang B, Liu Y, Hu Q. 2016. DC-SIGN as an attachment factor mediates Japanese encephalitis virus infection of human dendritic cells via interaction with a single high-mannose residue of viral E glycoprotein. Virology 488:108–119. https://doi.org/10.1016/j.virol.2015.11.006.

57. Khoo US, Chan KY, Chan VS, Lin CL. 2008. DC-SIGN and L-SIGN: the SIGNs for infection. J Mol Med (Berl) 86:861–874. https://doi.org/10.1007/s00109-008-0350-2.

58. Jaeger A, Murrieta RA, Goren L, Crooks C, Moriarty R, Weiler A, Rybarczyk S, Semler M, Huffman C, Mejia A, Simmons H, Fristsch M, Osorio J, O'Connor S, Ebel G, Freidrich T, Aliota MT. 2018. Zika viruses of both African and Asian lineages cause fetal harm in a vertical transmission model. BioRxiv https://doi.org/10.1101/387118.

59. Hanna SL, Pierson TC, Sanchez MD, Ahmed AA, Murtadha MM, Doms RW. 2005. N-linked glycosylation of West Nile virus envelope proteins influences particle assembly and infectivity. J Virol 79:13262–13274. https://doi.org/10.1128/JVI.79.21.13262-13274.2005.

60. Garcia-Vallejo JJ, van Kooyk Y. 2013. The physiological role of DC-SIGN: a tale of mice and men. Trends Immunol 34:482–486. https://doi.org/10.1016/j.it.2013.03.001.

61. Michlmayr D, Andrade P, Gonzalez K, Balmaseda A, Harris E. 2017. CD14(+)CD16(+) monocytes are the main target of Zika virus infection in peripheral blood mononuclear cells in a paediatric study in Nicaragua. Nat Microbiol 2:1462–1470. https://doi.org/10.1038/s41564-017-0035-0.

62. Foo SS, Chen W, Chan Y, Bowman JW, Chang LC, Choi Y, Yoo JS, Ge J, Cheng G, Bonnin A, Nielsen-Saines K, Brasil P, Jung JU. 2017. Asian Zika virus strains target CD14(+) blood monocytes and induce M2-skewed immunosuppression during pregnancy. Nat Microbiol 2:1558–1570. https://doi.org/10.1038/s41564-017-0016-3.

63. Domínguez-Soto A, Sierra-Filardi E, Puig-Kröger A, Pérez-Maceda B, Gómez-Aguado F, Corcuera MT, Sánchez-Mateos P, Corbí AL. 2011. Dendritic cell-specific ICAM-3-grabbing nonintegrin expression on M2-polarized and tumor-associated macrophages is macrophage-CSF dependent and enhanced by tumor-derived IL-6 and IL-10. J Immunol 186:2192–2200. https://doi.org/10.4049/jimmunol.1000475.

64. Navarro-Sanchez E, Altmeyer R, Amara A, Schwartz O, Fieschi F, Virelizier J-L, Arenzana-Seisdedos F, Desprès P. 2003. Dendritic-cell-specific ICAM3-grabbing non-integrin is essential for the productive infection of human dendritic cells by mosquito-cell-derived dengue viruses. EMBO Rep 4:723–728. https://doi.org/10.1038/sj.embor.embor866.

65. Gong D, Zhang TH, Zhao D, Du Y, Chapa TJ, Shi Y, Wang L, Contreras D, Zeng G, Shi PY, Wu TT, Arumugaswami V, Sun R. 2018. High-throughput fitness profiling of Zika virus E protein reveals different roles for glycosylation during infection of mammalian and mosquito cells. iScience 1:97–111. https://doi.org/10.1016/j.isci.2018.02.005.

66. Hamel R, Dejarnac O, Wichit S, Ekchariyawat P, Neyret A, Luplertlop N, Perera-Lecoin M, Surasombatpattana P, Talignani L, Thomas F, Cao-Lormeau V-M, Choumet V, Briant L, Desprès P, Amara A, Yssel H, Missé D. 2015. Biology of Zika virus infection in human skin cells. J Virol 89:8880–8896. https://doi.org/10.1128/JVI.00354-15.

67. Goo L, DeMaso CR, Pelc RS, Ledgerwood JE, Graham BS, Kuhn RJ, Pierson TC. 2018. The Zika virus envelope protein glycan loop regulates virion antigenicity. Virology 515:191–202. https://doi.org/10.1016/j.virol.2017.12.032.

68. Perera-Lecoin M, Meertens L, Carnec X, Amara A. 2013. Flavivirus entry receptors: an update. Viruses 6:69–88. https://doi.org/10.3390/v6010069.

69. Agrelli A, de Moura RR, Crovella S, Brandão LAC. 2019. ZIKA virus entry mechanisms in human cells. Infect Genet Evol 69:22–29. https://doi.org/10.1016/j.meegid.2019.01.018.

70. Sirohi D, Kuhn RJ. 2017. Zika virus structure, maturation, and receptors. J Infect Dis 216:S935–S944. https://doi.org/10.1093/infdis/jix515.

71. Pierson TC, Diamond MS. 2012. Degrees of maturity: the complex structure and biology of flaviviruses. Curr Opin Virol 2:168–175. https://doi.org/10.1016/j.coviro.2012.02.011.

72. Sirohi D, Chen Z, Sun L, Klose T, Pierson TC, Rossmann MG, Kuhn RJ. 2016. The 3.8 A resolution cryo-EM structure of Zika virus. Science 352:467–470. https://doi.org/10.1126/science.aaf5316.

73. de Alwis R, Williams KL, Schmid MA, Lai CY, Patel B, Smith SA, Crowe JE, Wang WK, Harris E, de Silva AM. 2014. Dengue viruses are enhanced by distinct populations of serotype cross-reactive antibodies in human immune sera. PLoS Pathog 10:e1004386. https://doi.org/10.1371/journal.ppat.1004386.

74. Brien JD, Lazear HM, Diamond MS. 2013. Propagation, quantification, detection, and storage of West Nile virus. Curr Protoc Microbiol 31:15D.3.1–15D.3.18. https://doi.org/10.1002/9780471729259.mc15d03s31.

75. Oliphant T, Nybakken GE, Engle M, Xu Q, Nelson CA, Sukupolvi-Petty S, Marri A, Lachmi BE, Olshevsky U, Fremont DH, Pierson TC, Diamond MS. 2006. Antibody recognition and neutralization determinants on domains I and II of West Nile Virus envelope protein. J Virol 80:12149–12159. https://doi.org/10.1128/JVI.01732-06.

76. Messer WB, Yount B, Hacker KE, Donaldson EF, Huynh JP, de Silva AM, Baric RS. 2012. Development and characterization of a reverse genetic system for studying dengue virus serotype 3 strain variation and neutralization. PLoS Negl Trop Dis 6:e1486. https://doi.org/10.1371/journal.pntd.0001486.

77. Smith SA, de Alwis AR, Kose N, Harris E, Ibarra KD, Kahle KM, Pfaff JM, Xiang X, Doranz BJ, de Silva AM, Austin SK, Sukupolvi-Petty S, Diamond MS, Crowe JE, Jr. 2013. The potent and broadly neutralizing human dengue virus-specific monoclonal antibody 1C19 reveals a unique cross-reactive epitope on the bc loop of domain II of the envelope protein. mBio 4:e00873-13. https://doi.org/10.1128/mBio.00873-13.

78. Henchal EA, Gentry MK, McCown JM, Brandt WE. 1982. Dengue virus-specific and flavivirus group determinants identified with monoclonal antibodies by indirect immunofluorescence. Am J Trop Med Hyg 31:830–836. https://doi.org/10.4269/ajtmh.1982.31.830.

79. Lai CY, Tsai WY, Lin SR, Kao CL, Hu HP, King CC, Wu HC, Chang GJ, Wang WK. 2008. Antibodies to envelope glycoprotein of dengue virus during the natural course of infection are predominantly cross-reactive and recognize epitopes containing highly conserved residues at the fusion loop of domain II. J Virol 82:6631–6643. https://doi.org/10.1128/JVI.00316-08.

80. Lanciotti RS, Kosoy OL, Laven JJ, Velez JO, Lambert AJ, Johnson AJ, Stanfield SM, Duffy MR. 2008. Genetic and serologic properties of Zika virus associated with an epidemic, Yap State, Micronesia, 2007. Emerg Infect Dis 14:1232–1239. https://doi.org/10.3201/eid1408.080287.